A CNN-Based Surrogate Model to Estimate the 2-D and 3-D Core Power Distributions in i-SMR

Jung Seok Kwon [a], Tongkyu Park [a*], Sung-kyun Zee
[a]*FNC Technology, Headquarters, 13 Heungdeok 1-ro,*
Giheung-gu, Yongin-si, Gyeonggi-do, 16954, Republic of Korea
[*]*Corresponding author: tongkyu@fnctech.com*

***Keywords :** reactor physics, core power distribution, convolution neural network, flexible operation, i-SMR

1. Introduction

To achieve global net zero greenhouse gas emissions, the power system's decarbonization has become increasingly important. Nuclear power is one of the major options to achieve carbon neutrality because of its low carbon footprint. In Korea, the i-SMR project has been in progress, focusing on improved safety and operational flexibility compared to conventional commercial light-water reactors [1],[2].

Due to the high variability and limited controllability of renewable energy sources, fossil-fuel-based power sources have been used to ensure the supply-demand balance of the power grid because of their flexibility.[3] The flexible operation of nuclear power can reduce the share of carbon-based power sources while preventing the curtailment of renewable energy sources. Additionally, it can help reduce the operational and maintenance (O&M) costs of the entire power system.[4]

However, there are already several obstacles that make flexible operation difficult. Examples of nuclear design include identifying optimal in-core loading patterns for flexible operation and defining the appropriate control rod positions for power adjustments during load-following operations.

Conventional commercial nuclear power plants (NPPs) have typically served as the base load of power systems. Their control rods were used to perform emergency power control and shutdown procedures.

In the case of i-SMR intended for flexible operation, control rods serve as mechanical shims. Furthermore, because soluble boron is not present, burnable absorbers must compensate for its lack, which uniformly suppresses reactivity within the core.

These design features have resulted in a significant increase in the number of loading pattern (LP) cases that require analysis, demanding a speed up of the core analysis process.

As AI technology has advanced, we now meet a variety of AI-based applications in our daily lives. Additionally, user-friendly machine learning frameworks have made it easy for non-experts to incorporate AI into their domains without requiring extensive AI knowledge. Among AI techniques, CNN is a specialized neural network for vision tasks. It serves a fundamental network in various domains, including object detection, segmentation, recognition, and image generation. Also, CNN have been used in core analysis. Some cases have utilized CNN to reconstruct core power distribution using core measurement data [5-7].

To speed up the loading pattern optimization process, several surrogate models were developed to predict core parameters. C. Wan et al. developed the CNN-based surrogate model and integrated with genetic algorithm[8]. In other cases, surrogate models were developed to be integrated with simulated annealing algorithm that includes screening technique[9-11]. This screening technique conditionally accept the results from surrogate model based on the probability distribution.

Regarding the prediction of power distribution without in-core measurement data, there has been research focused on predicting the position and value of pin power peaking factor (PPPF). In this study, 26 (24+2) axial layers were simplified into three regions, and form functions were used to enable the neural network to process the power distribution. Finally, the model outputs the assembly-wise power distribution, represented as 8x8x1[12].

In this paper, we present a surrogate model to accelerate the analysis of power distribution within the core. The training dataset was produced using the ASTRA core design code, and our CNN model was trained on it. The model predicted both pin-wise 2-D power distribution and assembly-wise 3-D power distribution.

2. Methodology

We used our surrogate model to do core analysis on the i-SMR design specification. Fuel composition types were classified into eight categories based on gadolinium enrichment, burnable rod arrangement, and the number of burnable rods within each composition. The number of burnable absorber rods that could be put in each composition was either 0, 12, 16, 20, 24, or 28. We only used the A type fuel batch, which was loaded in the first cycle of the core.

2.1. Data Preparation

The ASTRA core design code generated a total of 37,532 data points. Of these, 32,089 were used to train the model, 3,754 for testing, and 1,689 for validation during the training process. we only produced the

training dataset for the beginning of the cycle (BOC) and evaluated the model's performance. The model was developed to collect two sorts of input data. The primary input, also known as the main-input, was created utilizing the loading pattern and the matching nuclear cross-section of the fuel batches.

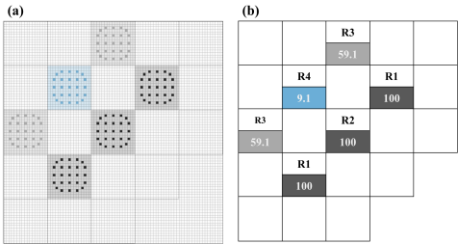

Fig. 1 Control rod position map for **(a)** pin-wise 2-D power and **(b)** assembly-wise 3-D power distribution.

The sub-input type differed between the 2-D and 3-D prediction cases. The sub-inputs in the 2-D case included the form function, enrichment map (uranium and gadolinium enrichment), and pin-wise control rod map (see Fig.1). In the 3-D case, only the assembly-wise control rod map was considered as a sub-input.

2.2. Pin-wise 2-D Power Distribution

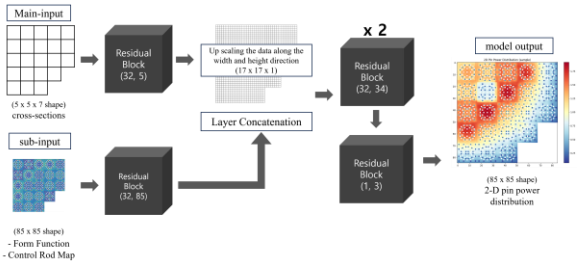

Fig. 2 Model architecture for 2-D pin-wise power distribution.

The main-input data structure was a 3-D tensor of 5x5x7, with the last dimension of 7 representing two group cross-sections. The sub-input data was an 85x85 matrix. During the training process, each cell of 5x5 matrix of the main input was upscaled horizontally into 17x17 before being concatenated with the sub-input data.

The residual block consisted of two parts. The first part contained two convolutional layers, while the second part was a shortcut layer. The first convolutional layer had the filter and kernel values from residual block. For example, if the residual block has parameters of (32, 5), the convolutional layer processes the tensor with 32 filters and a 5x5 kernel. After that, the tensor passes through another convolutional layer with 32 filters and a 1x1 kernel. The second part of the block was the shortcut layer. The input tensor to the residual block is fed into this layer, which has 32 filters and a 1x1 kernel. Finally, the outputs of the two parts are added together. The output form of the model was 85x85 pin power distribution. The architecture of the model is depicted on Figure 2.

2.3 Assembly-wise 3-D Power Distribution

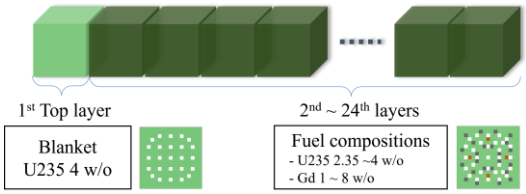

Fig. 3 Example of axial configuration of fuel batches.

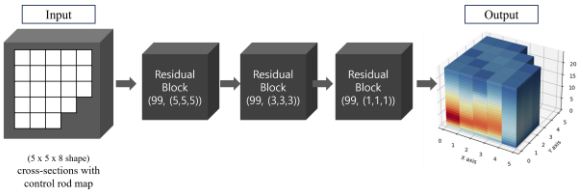

Fig. 4 Model architecture for 3-D assembly-wise power distribution.

Each fuel batch assembly was consisted of 24 layers of fuel composition. The top layer of the A type batch was covered by a blanket made up of only 4 w/o U-235 fuel rods and blank holes for control rods. The remaining 23 layers consisted of the same fuel compositions, which contained gadolinium burnable absorbers. Each composition had its own nuclear cross-sections. The main input data consists of 4-D tensors with dimensions 24x5x5x7, representing an array of 3-D tensors. The input tensor passes through residual blocks composed of 3D convolution layers, finally producing an output with dimensions 24x5x5x1.The architecture of the model is depicted on Figure 4.

3. Results

Table I: Errors of 2-D Pin Power Prediction

Relative Error	FF with Rod position	Form Function
Global mean	0.821%	1.388%
Maximum mean error per LP	2.018%	4.363%
Global max	73.532%	100.000%
Averaging max error per LP	10.787%	20.354%
Global mean of Peak value prediction	0.462%	0.846%
Global max of Peak value prediction	3.393%	5.677%

We examined performance improvements with and without control rod data. Tables I and II present the prediction error results for 2-D pin power distribution and 3-D assembly-wise power distribution respectively.

In both 2-D and 3-D models, adding control rod data reduced prediction errors across all the criteria.

Table II: Errors of 3-D Assembly-wise Power Prediction

Relative Error	with Rod position	only main-input used
Global mean	2.080%	2.296%
Max of mean	6.959%	11.474%
Global max	42.525%	113.106%
Mean of max	11.522%	28.007%
Global mean of Peak value prediction	1.660%	4.761%
Global max of Peak value prediction	12.173%	33.251%

4. Discussion

4.1. Error analysis of 2-D Power Distribution

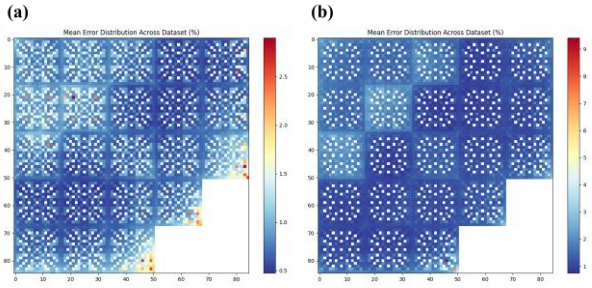

Fig. 5 Global mean error distribution of pin-wise 2-D power distribution (a) with control rod map and (b) without rod data.

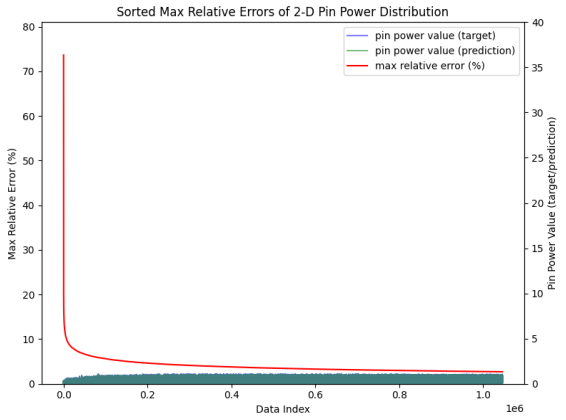

Fig. 6 Sorted relative max errors of 2-D pin power distribution (form function with control rod map data)

Fig. 5 shows the global accumulated mean error distribution. The error distribution was calculated by averaging the error values across all datasets for each pin location. The left side of the plot depicts the inclusion of control rod data, whereas the right side depicts the usage of only the form function. Note that the two plots have different scales. The maximum value on the left side is approximately 3, whereas on the right side it is around 9.

Fig. 6 shows the plot of examined maximum error, target power values, and predicted power values for each data point of the 2-D pin power distribution. The global maximum error was 73.532%, although the majority of errors were less than 5% over the whole dataset.

Additionally, we investigated the sources of the large maximum errors. It was found that in all cases, the neural network predicted values lower than the already low target power values (e.g., predicting a power value of 0.1 as 0.02), causing large relative errors. Core power values in the periphery of the core region are relatively lower than those in other parts of the core region. This is supported by the observation of substantial relative errors in the peripheral regions of the core, as shown in Fig. 5.

4.2. Error analysis of 3-D Power Distribution

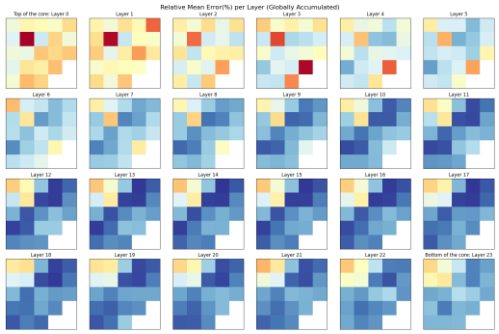

Fig. 7 Plane-wise relative mean error distribution of 3-D power distribution.

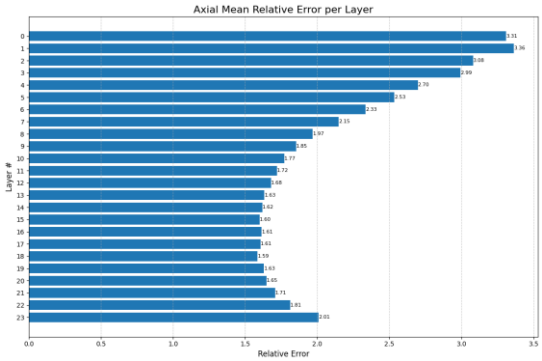

Fig. 8 Axial relative mean error of 3-D power distribution.

In Figure 7, we show the global plane-wise error distribution for 3-D assembly-wise prediction. In the axial direction, considerably high inaccuracy was noticed on the top side of core. In the horizontal directions, the location where the rod bank R4 is inserted has a higher inaccuracy than any other location of LP. The placement of the R4 rod bank is shown on right side of Fig.1.

4.3. Comparison with related work

Previous study [12] utilized 3D convolutional layers to predict the assembly-wise PPPF. In that study, 26 (24+2) axial layers were divided into three regions, with an input shape of 3x17x17x5. The final output of the model was either an 8x8x1 assembly-wise power distribution or a 1x1x1 PPPF value.

In contrast, this paper did not simplify the axial layers into three regions. Instead, we used all 24 layers directly as input, producing a 3D power distribution output for the assemblies that encompasses all 24 layers. Unlike the previous study [12], which used a form function as an input to identify the PPPF value and location, we did not incorporate a form function. This is a preliminary investigation to validate the potential for predicting 3D assembly-wise power distribution, and the model was not optimized. Form functions and detailed pin-wise information are planned for future work on 3D pin-wise power distribution prediction."

5. Conclusion

We performed 2-D and 3-D power distribution predictions for the BOC of the initial core, achieving good accuracy and demonstrating the ability to speed up core analysis. For 2-D pin power prediction, each pin point's relative error was less than 1%. Regarding computation time, the model took 5 seconds to predict 3,754 loading pattern (LP) cases, or 1.3 milliseconds per case. We also confirmed that there is room for more research on 3-D power prediction. In the 2-D pin power distribution, the highest relative error is 73.532%. We conducted a thorough of our results, sorting them by high error values in the 2-D pin power case. The model underestimated lower target power values for cases that exceeded the 7% error threshold; no instances of overestimating high power values were noted.

Regarding the pin-wise peak power prediction, we were able to obtain a global maximum of 3.393% and a relative mean error of 0.462%.

With additional research and improvements, the model is expected to accelerate the reactor design process and provide guidelines for load-following operation through its inherent rapid computational speed.

ACKNOLEDGEMENTS

This work was supported by the Innovative Small Modular Reactor Development Agency grant funded by the Korea Government (MOTIE) (RS-2023-00259289)

REFERENCES

[1] J.I. Lee, Review of Small Modular Reactors: Challenges in Safety and Economy to Success. *Korean Journal of Chemical Engineering*, 2024, 1-20.

[2] H.O. Kang, B.J. Lee, S.G. Lim, Light water SMR development status in Korea. *Nuclear Engineering and Design*, 2024, 419: 112966.

[3] G. Strbac, et al. Decarbonization of electricity systems in Europe: Market design challenges. *IEEE Power and Energy Magazine*, 2021, 19.1: 53-63.

[4] J.D. Jenkins, et al. The benefits of nuclear flexibility in power system operations with renewable energy. *Applied energy*, 2018, 222: 872-884.

[5] H. Xia, B. Li, and J. Liu Research on intelligent monitor for 3D power distribution of reactor core. *Annals of Nuclear Energy*, 2014, 73: 446-454.

[6] A. Pirouzmand, M.K. Dehdashti, Estimation of relative power distribution and power peaking factor in a VVER-1000 reactor core using artificial neural networks. *Progress in Nuclear Energy*, 2015, 85: 17-27.

[7] W. Li, et al. Artificial neural network reconstructs core power distribution. *Nuclear Engineering and Technology*, 2022, 54.2: 617-626.

[8] C. Wan, K. Lei, and Y. Li. "Optimization method of fuel-reloading pattern for PWR based on the improved convolutional neural network and genetic algorithm." *Annals of Nuclear Energy* 171 (2022): 109028.

[9] K. Park, T. Park, S. Zee, B.S. Koo, Convolutional Neural Network Applied Core Peaking Factor Analysis and Sensitivity Study for SMART Core. In: *Transactions of the Korean Nuclear Society Autumn Meeting, Online*. 2020.

[10] J. Kwon, T. Park, and S. Zee. "AI-Based Prediction Module of Key Neutronic Characteristics to Optimize Loading Pattern for i-SMR with Flexible Operation." *Korean Journal of Chemical Engineering* (2024): 1-19.

[11] H. Jang, et al. "Prediction of OPR-1000 Neutronic Design Parameters Using Convolutional Neural Network for Fuel Loading Pattern Optimization." *Transactions of the Korean Nuclear Society Virtual Autumn Meeting December 17-18* (2020)

[12] Y.D. Nam, J. Y. Lee, and H. J. Shim. "Convolutional neural network for BOC pin power prediction." Transactions of the Korean Nuclear Society Spring Meeting Jeju, Korea, May 23-24, (2019)